20 years of active deformation on volcano caldera: Joint analysis of InSAR and AInSAR techniques

Brunori C.A.[1], Bignami C.[1]; Stramondo S. [1], Bustos E. [2,3]

1 Istituto Nazionale di Geofisica e Vulcanologia (Roma, Italy)

2 National University of Salta (Argentina).

3 Consejo Nacional de Investigaciones Científicas y Técnica (Argentina).

Abstract

InSAR (Interferometric Synthetic Aperture Radar) techniques are applied to investigate last two decades of surface deformation of the Cerro Blanco/Robledo Caldera (CBRC). The objective is the identification of deforming patterns that alter the shape of these complex structures when they show low or null activity. The joint analysis between results by using different methods over a long time span, represents a unique opportunity to improve knowledge of volcanic structures located in remote area and, for this, poorly or not monitored.

In this work we identify displacement patterns over the volcanic area, by using both classical differential InSAR analysis, and A-InSAR (Advanced InSAR) analysis based on SAR data acquired by ERS-1/2 and ENVISAT sensors during the 1996–2010 time interval,. The satellite-derived information allows us to characterize the deformation pattern that affected the CBRC and shows that the actively deforming CBRC is subsiding in the observed period. In order to figure out the deformation history of CBRC, we analyzed the four sub-periods 1992-1996, 1996-2000, and 2005-2010 by using standard differential InSAR technique, and the interval 2003-2007 by adopting an A-InSAR technique.

Subsidence velocities of the CBRC caldera are about 2.6 cm/yr in the time interval 1992-1996 (measured with ERS descending data), 1.8 cm/yr in 1996-2000 (ERS descending data), 1.2 cm/yr in

2003-2007 (ENVISAT descending data),and finally, 0.87 cm/yr in 2005-2010 (ENVISAT ascending data). Moreover, outside the caldera and in particular in the NW area, we observe the presence of positive velocity values. Results show that: a) a decreasing subsidence rate might be related to the reduction of volcanic activity in correspondence of the CBRC; b) positive velocity signal, decreasing with time, might be interpreted as follows: - evidence of volcano structure lateral spreading, according to the velocity pattern distribution in this area and to the relative local flanks topographic convexity of the volcano structure; - uplift signal of this sector of mountain chain; - combination of the two mechanisms above.

Keywords:

InSAR; Deflation; Calderas; Volcanic structures;

1. Introduction

Calderas are roughly circular ground depressions and are distinctive features in volcanic areas. They appears as very large morphological structures which may arise by the coalescence of several small craters formed after repeated explosion, collapse, or the stopping of surface rocks by a large underground magma chamber. Such depressions are near-ubiquitous features of volcanic structures, and they occur in association with volcanism of all compositions and in all regional tectonic settings (Holohan et al., 2011; Newhall and Dzurisin, 1988).

The Cerro Blanco-Robledo Volcanic Complex, located in Catamarca province (northwest Argentina, 26°45'S- 67°44'W - Fig. 1a-b), is the youngest caldera in the Southern Central Andes (0.1 Ma; Arnosio et al. 2008). The Smithsonian Institute's database names the whole volcanic structure simply Robledo (Simkin and Siebert, 1994). de Silva and Francis (1991) refer to the silicic dome in the western part of the caldera as Cerro Blanco. Hereafter, for simplicity and completeness, and according to Arnosio et al. (2005), we use "Cerro Blanco/Robledo Caldera" (CBRC) for the whole structures which includes two 4-5 km wide coalescent circular features (NW Cerro Blanco and SW Robledo caldera), the western crystalline Cerro Blanco dome and up to the NW El Niño volcanic structure (Fig 1b.). As first hypothesis, we can consider part of the CBRC the roughly circular structure enveloping the above mentioned structures (about 12 km in diameter).

The CBRC case study has no hazardous characteristics because located in an uninhabited region. Its environmental conditions (arid climate, relative low elevation gradients and absence of vegetation) can be considered as a natural laboratory for the application of satellite remote sensing microwave techniques. Here we infer deformations caldera signals, associated with the present-day volcanic activity, by using standard differential Interferometric Synthetic Aperture Radar (InSAR) techniques and multitemporal or Advanced InSAR (A-InSAR). In particular we exploit

time series analysis obtained by the software package Stamps-MTI (Stanford Method for Persistent Scatterers – Multi Temporal InSAR; Hooper et al., 2008).

Finally, we present new geodetic measurements of ENVISAT satellite SAR images of CBRC area between 2003 and 2010. The application of both InSAR and A-InSAR techniques allowed us to estimate the entity and the geometry of caldera deflation (velocity of this deformation in the time). We also try to interpret the detected signals as evidences of shallows and/or deep mechanisms responsible for these phenomena.

2. What's a caldera?

In order to define from a morphological and volcanological point of view the natural object that we are studying, we are looking for a definition of "caldera" and the possible features recognizable in the CBRC area. The "Encyclopedia of Volcanoes" (Sigurdsson and al. eds., 2000), provides different definitions for "calderic structures", such as: large volcanic depressions, more or less circular in shape, the diameter of which is many times greater than that of included vents; crater or surface depression resulting from collapse of an underlying magma; chamber roof during withdrawal of magma; features previously described as ‘‘cauldrons,’’ which are considered to represent deeper erosive levels of the same fundamental structures and igneous processes; summit crater of a volcano; collapse depression found over a subsurface magma chamber; circular or irregular collapse feature formed over the evacuated magma chamber within a volcano; etc…

All these definitions refer to the product resulting from the volcanic edifices explosion and/or implosion. According to Borgia et al. (2010), we consider as caldera a "geologic environment that, at any scale, is characterized by three linked elements: magma, eruptions and edifice", and by

assuming these morpho-structures as one of the possible stages, in volcanic environment, of the magmatic cycle (Sheridan and Wohletz, 1983; Dzurisin, 2003).

Large-scale explosive eruptions yielding greater than 10^{15} kg of products (>150 times the mass of the 1991 eruption of Mt. Pinatubo), like those producing caldera-forming, are historically rare (Manson et al., 2004). Despite their low frequency, the associated pyroclastic flows tend to travel distances of several tens of kilometers in any direction from the crater. The evaluation of the next stages of the evolution of calderas, such as eruptions or slow or fast inflation and/or deflation of the structures, is carried on through a long time and continuous volcanological monitoring. Calderas structure undergo periods of unrest highlighted by ground displacement, seismicity, and gas emissions and are some of the most studied volcanic features particularly for their possible implications for hazard assessment and mitigation (Lundgren et al., 2001; Lanari et al., 2004; Kwoun et al., 2006; Wicks et al., 2006; Chang et al., 2010; Vilardo et al., 2010; Aguirre-Diaz et al., 2011; Holohan et al., 2011 and references therein). Collapsed calderas are among the most investigated geological objects also because of their association with economic deposits and geothermal energy (Costa, 2008).

3. The CBRC

Principal characteristic of the CBRC is its uniqueness among the actively deforming volcanoes because it is subsiding (Pritchard and Simons, 2004; Viramonte et al., 2005a). The CBRC is located at the southern limit of the Central Andes (26 ° 45 'LS - 67 ° 45' LW). It consists of ignimbrites, fall deposits and domes associated with a nested system of calderas. The CBRC is located on La Hoyada Volcanic Complex FIG 1b, which consist in volcanic rocks, pyroclastic and volcaniclastic rocks of Miocene age, and on lower Paleozoic basement rocks. The CBRC eruptive history can be

reconstructed in two stages (Arnosio et al., 2008) based on stratigraphy, geochronological (Ar / Ar sanidine; Viramonte et al, 2008) and geochemical data. The first one, represented by a widespread ignimbrite named Campo de la Piedra Pómez (~ 73 ± 23.2 ka) that reached a distance more than 50Km from the CBRC (FIG 1b).The volcanic structure, from which it was issued this unit, is not clearly defined. However, from lateral facies variations and anisotropy of magnetic susceptibility (AMS) data (Baez et al., 2011), it follows that the location of it would be within the CBRC. The second stage comprises of Purulla and El Medano ignimbrite units (22 and 12 ka) associated with the Cerro Blanco caldera and possibly Robledo caldera (Arnosio et al., 2008). After the CBRC collapse, the volcanic activity developed along a 60°N oriented structure. The last activity was characterized by phreatic and phreatomagmatic eruptions into the caldera depression where the 60°N fault system intersects a 140°N fault system (Arnosio et al., 2005, 2008). Viramonte et al. (2005 a) assume that these two main fault systems were responsible and controlled the volcanic complex eruptions and the CBRC forming. The last eruption dates back 5000 years ago (Montero Lopez, 2010). More recently a thermal anomaly has been detected in the centre of the Caldera (Arnosio et al, 2008; Viramonte et. al, 2005a).

[Figure 1]

Pritchard & Simmons (2004) performed a DInSAR survey of the remote central Andes volcanic arc between the years 1992 and 2002 with ERS-1 and ERS-2 satellite radar images. They found CBRC is subsiding with an average velocity of 2–2.5 cm/yr along the satellite line of sight (LOS). The rate of subsidence seems to decrease with time from a maximum of more than 2.5 cm/yr in the radar LOS (interferograms spanning 1992 - 1996/7) to less than 1.8 cm/yr (1996 - 2000). Authors suppose that the subsidence can be related to the observed hydrothermal activity or to the cooling and crystallization of magma chamber.

To validate the data obtained by Pritchard & Simmons (2002, 2004), Viramonte et al. (2005b) conducted both seismic and geodetic experiments. In February 2004 a network of 5 broadband digital seismometers was installed in Cerro Blanco area. In April 2004 and February 2005, high-precision GPS network (with 5 benchmarks) was installed. The first results of this GPS campaign show a signal of subsidence process which is larger at the centre of the caldera structure. Values of approximately 1.4 cm/yr were obtained. A further gravimetric study of CBRC has also been realized to improve the structural knowledge of this area (De Filippo et al., 2008). Results revealed a low gravity caldera collapse structure. The study identifies the top basement (pre-volcanic) and its relationship with the overlaying volcanic deposits. They found that the pre-volcanic basement appears very disjointed indicating a probable piecemeal type caldera structure. Arnosio et al. (2005) observe that the geothermal field, the phreatomagmatic craters and the subsidence suggest that CBRC piecemeal structure is in a resting phase. Moreover, they suppose that the CBRC could represent one of the events of multiphase collapse of a much larger structure.

4. Volcanic structures monitoring by means of InSAR techniques

In order to understand the acting volcanic processes, it is vitally important to monitor and to measure the subtle changes visible at the surface using modern instrumentation (Berrino et al., 1992, Geyer and Martí, 2009). Studies of unrest at calderas, often with attendant geothermal and mineralizing systems provide valuable information on the development of ancient systems, now deeply eroded. Most of caldera unrest involves a series of interactions between the local tectonic stress field, the sub-caldera magma chamber, and groundwater (Newhall and Dzurisin, 1988). Monitoring these interactions can improve our understanding of the way in which calderas behave and respond to variations in the local stress regime and in the supply of magma from depth. In

summary, it is essential to know the evolution of volcanic structures movements, in order to understand deep phenomena that are the engine of these movements. As for the hundred of remote volcanic structures worldwide, InSAR is currently the most viable way to establish the background level of activity.

SAR Interferometry is an imaging technique for measuring the topography, its changes over time, and other changes in the characteristics of the Earth surface. By exploiting the phase component of the SAR signal, interferometry has achieved a central role in Earth Sciences. Indeed, InSAR provides a synoptic view of the investigated area where the surface displacements are measured over the whole image with unprecedented accuracy. Thanks to its properties InSAR can be applied in cartography, geodesy, land cover characterization, and natural hazards (Rosen et al., 2000), seismic and volcanic risk in particular. InSAR has shed some light on what volcano structures do when they are not erupting (Dzurisin, 2003).

For rapid and big volume changes, which correspond to volumes erupted during most hazardous eruptions, surface deformations should be measurable even with classical geodetic instruments that are widely used for volcano monitoring (e.g. theodolite, electronic distance meter, bubble tiltmeters, etc.). Conversely, during typically log rest period when no or small deformation takes place, the temporal resolution of most geodetic datasets is inadequate. Moreover, some of these monitoring techniques are not sufficiently accurate to detect small surface changes preceding many eruptions, or provide only punctual information (e.g. GPS measurements). In short, the complete characterization of volcano structures deformation requires that measurements should be made in the right place, at the right time, and with adequate precision, challenging topics using conventional geodetic techniques (Dzurisin, 2000). Satellite InSAR techniques can support, and in some cases overcome, the limitations of traditional geodetic techniques and can integrate the deformation signals for geophysical monitoring in general, and for volcanic complexes in

particular. Indeed, this space imaging technique can provide regional and spatially continuous measurements of surface displacements, and can be easily applied for remote regions where natural or political drawbacks may limit the possibilities to work on site.

Despite the ability of InSAR techniques to monitoring crustal movement at surface, their capability remains, in some cases, limited. Many vulnerable places such as volcanic inhabited areas, are located in regions where climatic conditions, vegetation coverage and water resources, produce optimal conditions in terms of human presence, but conversely can have negative impact on the InSAR and A-InSAR applicability (Zhou et al., 2009). Indeed, environmental factors such as seasonal variability induce strong tropospheric artifacts on InSAR images (e.g. D'Oreye et al., 2010), while strong vegetated areas reflect on low SAR signal coherence as well as small signal-to-noise ratio. These factors can reduce or in the worst case prevent the ability to distinguish ground permanent or semi-permanent deformations signal from other radiometric contributions (Massonnet et al., 1995; Zebker and Villasenor, 1992; Zebker et al., 1997; Massonnet and Feigl, 1998; Amelung et al.,2000; Hooper et al., 2012; Biggs et al., 2007; Pinel et al. 2010; Philibosian and Simons, 2011). Fortunately, in the CBRC area the above cited environmental conditions are favorable to the application of interferometric techniques.

4.1. CBRC InSAR data processing

Deformation measurement for CBRC has been performed using SAR images acquired by the ERS and ENVISAT satellites of the European Space Agency (ESA). ERS1/2 and ENVISAT satellite missions are equipped with SAR sensors working at the same frequency (C-band, 5.3 GHz) but with differences in the acquisition capabilities. Indeed, the SAR on board of ENVISAT platform is the successor of the ERS SAR, with enhanced potentiality in terms of operating modes: area coverage,

range of incidence angles, and polarization. The ENVISAT data used for this work are acquired in the same modality of the ERS SAR (the so called ERS-like mode). All the images are in VV polarization, with an incidence angle of 23° and a spatial resolution of 25 m per pixel. This allows to jointly analyze the results coming from the two sensors. In particular, we follow the aforementioned approaches: standard differential InSAR and A-InSAR. In both approaches we used the SRTM (Shuttle Radar Topographic Mission) 3-arc-second (90 m) DEM (Farr et al., 2007) to remove the topographic phase contribution. A time series analysis on ENVISAT data, covering the time period between April 2003 and January 2007 (see Tab. I), has been computed following the processing chain implemented in StaMPS-MTI method, by Hooper (2008). StaMPS-MTI allows to exploit two A-InSAR techniques, the PS technique (Ferretti et al., 2001) and the SBAS technique (Berardino et al., 2002), by combining these two approaches for extracting the deformation signal for a higher number of points and with an overall signal-to-noise ratio higher than each single technique. It reflects in more reliable results, especially when dealing with limited dataset like our case study. For this analysis, thirteen SAR scenes have been processed and we estimated the mean velocity fields and the deformation history of the CBRC.

[Table 1]

The result of StaMPS-MTI processing is shown in Fig.2. The retrieved map shows a distribution of negative, quasi circular, deformation pattern (movement away from the satellite in the line of sight - LOS), corresponding to a subsiding area centered in the ridge separating the northern Cerro Blanco caldera and the southern Robledo caldera. The deformation pattern does not seem to take into account the topographic geometries of the two calderas. The measured rate of subsidence has a maximum value of -1.2 cm/yr in the radar LOS. This latter, for descending ENVISAT data, is of about 23° off nadir and about -168° with respect to north. Note that the higher positive values (blue pixels) are present in those portion of the image where some phase jumps occurred during

the phase unwrapping process (e.g. steepest areas, and zones with very low interferometric coherence).

[Figure 2]

A further analysis has been performed to extend the results obtained from SAR time series. We calculate a new deformation map by applying standard InSAR processing to a pair of ENVISAT images acquired on August 3, 2005 and June 23, 2010 on ascending track (track 318). We adopted this different approach because for this dataset the number of available images between 2007 and 2010 is low and time series analysis cannot be applied.

Fig. 3 reports the deformation map obtained for this second analysis. We can argue that the deformation patter is still quasi circular and centered in the same location of the surface velocity map shown in Fig. 2. The maximum displacement is negative, i.e. we are in presence of subsidence, with a value of about -4.3 cm in LOS (i.e. 23° off nadir and about -12° with respect to north), which means that the corresponding linear velocity for this time span is equal to -0.87 cm/yr.

[Figure 3]

For seeking of completeness, a third computation of InSAR processing has been conducted for the same ERS satellite images used in the work of Pritchard and Simons (2004). Indeed, we used the SAR pair on descending track (track 239, same LOS of ENVISAT descending images), taken on May 16, 1996, and on October 12, 2000. In such time window we found a maximum deformation rate of -1.8 cm/yr which is, of course, in agreement with the results reported in Pritchard and Simons (2004). Differently from the previous deformation maps, the center of the circular pattern is after the ridge separating Cerro Blanco and Robledo calderas, towards south-east. From this

consideration and looking to the three maps, we can argue that the shape of the inferred deformation is changing during the analyzed period.

[Figure 4]

For better delineating the changes of the deformation pattern, we traced three transects. The first one is on the NW-SE direction to analyze the whole CBRC structure (A-A', Fig.5). Two additional transects have been traced orthogonally to the first one and crossing the Cerro Blanco caldera and the Robledo caldera (traces B-B' and C-C' respectively, Fig. 5) . We analyzed the three corresponding deformation profiles with respect to the related topography. Looking at the three profiles in Fig.5, the ERS2 dataset (first time period) shows that the maximum value of subsidence is located close to Robledo caldera (dashed line). The profile A-A' (upper panel in Fig. 5) highlights that for the second time period (ENVISAT A-InSAR analysis; points cloud) the maximum subsidence "moved" towards the center of CBRC and has lower values (in modulus). Note that in order to compare the velocity values derived from A-InSAR approach and the deformation values obtained from standard differential InSAR approach, we calculated the cumulative deformation by multiplying the LOS mean velocity for the 4.4 years of observation. The points cloud correspond to a buffer zone of about 500m around the transect. For the last time window (ENVISAT differential InSAR; dotted line) we observe that the maximum subsidence value is decreased and it is located in between the two calderas (profile A-A', figure 5). Two additional details can be found in profile A-A' (Fig.5). The first one concerns the small segment on the deformation profile of ENVISAT InSAR data, with negative concavity, positioned just below the Cerro Blanco Caldera. Our hypothesis is that this decreased deflation can be related to the hydrothermal activity which is located in the same area (Viramonte et al., 2005a). The second issue is the positive (uplift) deformation visible soon outside the CBRC (6-7 mm) in the area between EN and LP (Fig. 1 b), measured with ERS dataset, which is less pronounced (almost zero) for the A-InSAR points cloud, while for the last

time period, inferred by ENVISAT single interferogram, is negative. Profiles B-B' and C'C' (Fig. 5), show the signals of the subsidence in the two sub-structures of CBRC. These two profiles confirm the decreasing of subsidence velocity at CBRC for all SAR dataset. Outside the two caldera structures, there are no clear uplift signals as observed in the NW section of profile A-A', but we only observe a decreasing of the subsidence velocity as the distance increases from the CBRC center. (see Fig. 2, 3,and 4 for the distribution of the deformation patterns)[Figure 5]

5. Discussion

Ground deformations associated with the present-day volcanic activity have been measured using InSAR and A-InSAR techniques. The actively deforming CBRC is subsiding in the time interval 1992-2010. In order to better highlight the deformation history of CBRC, we further analyzed the four sub-periods 1992-1996, 1996-2000, 2003-2007, and 2005-2010, corresponding to the four InSAR and A-InSAR data processing. In Fig. 6 the maximum surface subsidence values measured in the CBRC of the four SAR products are reported in function of time. The plot clearly shows that the subsidence rate is decreasing during the entire observation period, from a maximum rate of -2.6 cm/yr to -0.87 cm/yr, almost linearly. It confirms the slowing down trend according the ERS measurements (Track 239, 1996-2000; Track 10, 1992-2000 and Track 10, 1992-1996; Pritchard et al. 2004). These observations seem to assess that the volcanic deforming activity is “shutting down” or the deflation deceleration can be considered as a stage of low energy before a new periods of a new restart or another kind of volcanic activity is beginning.

[Figure 6]

As far as the deformation pattern is concerned, the quasi-concentric geometry of velocity field, centered between Cerro Blanco and Robledo calderas, is confirmed from all our deformation products (Fig 2, 3 and 4) and transects. They suggest that, though the morphology is characterized

by coalescing circular structures, the CBRC deforming caldera probably consists on a single and wide physical structure, in agreement with Di Filippo et al. (2008).

Calderas subsidence usually is controlled by the influence of mechanisms involving cooling and solidification and/or migration of magma, regional extension and removal of hydrothermal or magmatic fluids with concomitant compaction (Newhall and Dzurisin, 1988). Hutnak et al., 2009 (among others) postulate that hydrothermal fluids may play a role in ground surface displacements of calderas and, to test the hypothesis, they carry out numerical simulations. They found that hydrothermal fluids circulation may help explaining some of the calderas deformation that has not culminated in magmatic eruptions. Several authors have proposed that tectonic activity controls caldera collapse and shallow magma movement in the central Andes (e.g., Riller et al., 2001).

Pritchard and Simons (2004), describing the subsidence at CBRC, argue that the tectonic extension and magma withdrawal are unlikely explanations for mechanism of deflation. Moreover, the rate of cooling, estimated by modeling the deformation of coupled magmatic/hydrothermal systems, is complicated because the calculations involve many unconstrained parameters. Further conclusions by Pritchard and Simons (2004) demonstrate that the dimension of the chamber producing the observed surface deformation pattern, would have a radius 17 km. This value would be unlikely too big if compared with inferred magma chamber as, for example, in the Long Valley caldera (McTigue, 1997). They infer a depth of deflation source of 9-14 km, comparable to Yellowstone (7-10 km; Chang et al., 2010) and deeper than Campi Flegrei caldera, 3 km (Vilardo et al., 2010 and references therein). This model is unfortunately influenced by the lack of quantitative knowledge of hydrothermal activity that restricts the ability to describe the source responsible for the observed deformation pattern at the CBRC.

As already introduced in previous section, an active geothermal area in the Cerro Blanco caldera has been evidenced by thermal anomalies, small fumaroles and mud volcanoes. It suggests the presence of a hydrothermal system that can contribute to increase the conductive cooling of deep magma bodies. Moreover, processing techniques on ASTER (Advanced Spaceborne Thermal Emission and Reflection Radiometer) images detect a thermal anomaly in the centre of the Caldera confirming the above mentioned hydrothermal activity (Viramonte et. al, 2005a).

Our A-InSAR velocity map (Fig. 2) shows that the positive velocity values around and, in particular as evidenced by the profile in profile A-A' (Fig 5), immediately at NW of the CBRC, could be referred by a uplifting trend measured along the satellite LOS. According to their relative position with respect to the CBRC (outside and near to the volcanic structure), they could be interpreted as possible signal of CBRC structure lateral spreading (Merle and Borgia 1996). However, this interpretation it is not clearly supported by required evidences, such as documented presence of a weak basal layer (Fig. 1a). This positive trend would be also confirmed by the presence of morphological features, like the trace of the valley at the northern edge of this area (see Fig.1b) that seems to be curved toward NW, and a slight convexity in the NW flank of the caldera structure (see profile A-A' in the Fig 5). Actually, it is not easy to find another explanation for the positive pattern of velocity, and the valley curvature could be the result of the emplacement of volcanic products coming from eruptive CBRC activity. The distribution of the velocity pattern and the decreasing rate of uplift which is compliant with the decreasing subsidence phenomenon of CBRC structure, would not seem to support mechanisms of expansion of the magmatic chamber and/or intrusion of magma bodies outside the borders of “actual” CBRC. This is in agreement with Pritchard and Simons (2004). In addition, this behavior can be referred to uplift signal of this sector of mountain chain or a combination of these two mechanisms (local lateral spreading and

uplift). This consideration is also supported by looking at the eastern sectors of the B-B' and C-C' profiles, where (as already mentioned) there are no evidences of positive displacements.

Despite these outcomes, further observations are needed to constraint satellite measurement and to validate our interpretations.

6. Conclusions

In this work, radar satellite measurements of the Cerro Blanco/Robledo Caldera are presented. We identify deformation patterns which highlight the altering of a caldera structure in a resting phase period. We get the result performing a deformation comparison between outputs of two different InSAR techniques, using acquisitions of different sensors over a long time span. This methodology represents a unique opportunity to improve knowledge of natural structures, such as a volcanic structures, poorly or not monitored, and located in remote and inaccessible areas.

The results show that in the time interval we investigated (1992-2010), the caldera is subsiding with decreasing velocity. Indeed, the average speed between 1992 and 1996/7 is more than 2.5 cm/yr and 1.8 cm/yr from 1996 to 2000, and in the time intervals 2003-2007, and 2005-2010 the velocity maps show that the mean velocity is up to 1.2 cm/yr and 0.87 cm/yr respectively. These InSAR-based observations seem to assess the reduction of volcanic activity. Moreover, the pattern of the observed deformation signals, suggests that the movement involves the CBRC as a unique structure. In the NW part outside the CBRC, a positive velocity field has been observed. This positive pattern could be ascribed to a local lateral spreading of the CBRC collapsed structure; in alternative,, it could be referred to the uplift of this sector of mountain chain or to the combination of the two mechanisms above.

7. Acknowledgements

This work has been partly supported by SIASGE Project, a CONAE (SAOCOM project), ASI and INGV collaborative initiative. SAR data have been provided by the European Space Agency through the cat-1 project C1P.6435. A special thank to Andrea Borgia, Guido Ventura and to Roland Burgmann for the fruitful discussions and suggestions. The first author thanks Dr. Paolo Trenta and the people of Centro Studi Città di Foligno (PG, Italy) for the kind and generous hospitality, fruitful for the completion of this work.

8. References

Aguirre-Diaz, G., Geyer, A., Martí, J. and Acocella, V., 2011. Improving and facilitating research on collapse. EOS, 92, 53 - 54.

Amelung, F., Jonsson, S., Zebker, H., Segall, P., 2000. Widespread uplift and ''trapdoor'' faulting on Galapagos volcanoes observed with radar interferometry, Nature, 407, 993 – 996.

Arnosio, M., Becchio, R., Viramonte, J.G., Groppelli, G., Norini G., Corazzato, C., 2005. Geología del Complejo Volcánico Cerro Blanco (26° 45' LS- 67° 45' LO), Puna Austral. 16º Congreso Geológico Argentino, La Plata., Actas 1: 851 – 858.

Arnosio, M., Becchio, R., Viramonte, J., Groppelli, G., Norini, G., Corazzato C., 2005. Geologia del Complejo Volcánico Cerro Blanco (26°45' S - 67°45' O). XVI Congreso Geológico Argentino, La Plata. II, 851 - 858.

Arnosio, M., Becchio, R., Viramonte, J. G., de Silva, S., Viramonte, J.M., (2008). Geocronología e isotopía del Complejo Volcánico Cerro Blanco: un sistema de calderas cuaternario (73-12Ka) en los Andes Centrales del Sur. 13 Congreso Geológico Argentino, Jujuy, 1, 134 - 135.

Berardino, P., Fornaro, G., Lanari, R., Sansosti, E., 2002. A new algorithm for surface deformation monitoring based on small baseline differential SAR interferograms. IEEE Trans. Geosci. Remote Sensing, 40, 11, 2375-2383.

Baez, W., Arnosio, M., Viramonte, J.G., 2011. Análisis de facies y estudio de la fábrica magnética en la ignimbrita Campo de la Piedra Pómez, Puna Austral: Implicancias en sus mecanismos de transporte y depositación. XVIII Congreso Geológico Argentino, Neuquén 2011

Berrino, G., Rymer, H., Brown, G.C., Corado, C., 1992. Gravity-height correlations for unrest at calderas. J. Volcanol. Geotherm. Res. 53, 11 - 26.

Biggs, J., Wright, T., Lu, Z., Parsons, B., 2007. Multi-interferogram method for measuring interseismic deformation: Denali Fault Alaska. GJI, 170, 1165 - 1179.

Borgia, A., Aubert, M., Merle, O., van Wyk de Vries, B., 2010. What is a volcano? Geological Society of America Special Papers, 470, p. 1-9, doi:10.1130/2010.2470(01).

Chang, W.-L., Smith, R. B., Farrell, J. M., Puskas, C., 2010. An extraordinary episode of Yellowstone caldera uplift, 2004–2010, from GPS and InSAR observations. Geophys. Res. Lett. 37, L23302, doi:10.1029/2010GL045451.

Costa, F., 2008. Residence times of silicic magmas associated with calderas. In: Caldera Volcanism: Analysis, Modelling and Response. Gottsmann J, Marti J (eds), Developments in Volcanology 10: 1 - 55.

De Silva, S.L., Francis, P.W., 1991. Volcanoes of the Central Andes, ed. Springer-Verlag, New York.

Di Filippo, M., Di Nezza, M., Colombi, A., Viramonte, J. G., Toro, B., 2008. Estructura gravimetrica del Complejo Volcanico Cerro blanco, Puna Austral, Argentina. XVII Congreso Geológico Argentino. Actas I: 203 - 204.

D'Oreye, N., Gonzalez, P., Shule,r A., Oth, A., Bagalwa, M., Ekström, G., Kavotha, D., Kervyn, F., Lucas, C., Lukaya, F., Osodundu, E., Wauthier, C., Fernandez, J., 2010. Source parameters of the 2008 Bukavu-Cyangugu earthquake estimated from InSAR and teleseismic data. GJI, 184 (2), 934 - 948.

Dzurisin, D., 2000. Volcano geodesy: Challenges and opportunities for the 21st century. Phil. Trans. R. Soc. Lond. A , 358, 1547 - 1566.

Dzurisin, D. 2003. A comprehensive approach to monitoring volcano deformation as a window on the eruption cycle, Rev. Geophys. 41(1), 1001, doi:10.1029/2001RG000107.

Farr, T. G., et al., 2007, The Shuttle Radar Topography Mission, Rev. Geophys., 45, RG2004, doi:10.1029/2005RG000183.

Ferretti, A., Prati, C., Rocca, F., 2001. Permanent scatterers in SAR Interferometry. IEEE Trans. Geosci. Remote Sensing, 39(1), 8 - 20.

Geyer, A., Martí, J., 2009. Stress fields controlling the formation of nested and overlapping calderas: Implications for the understanding of caldera unrest. Journal of Volcanology and Geothermal Research, 181, 185 - 195.

Holohan, E. P., Schöpfer, M. P. J., Walsh, J. J., 2011. Mechanical and geometric controls on the structural evolution of pit crater and caldera subsidence. J. Geophys. Res. 116, B07202, doi:10.1029/2010JB008032.

Hooper, A., Bekaert, D., Spaans, K., Arıkan, M., 2012. Recent advances in SAR interferometry time series analysis for measuring crustal deformation, Tectonophysics, 514 - 517, 1 - 13, doi:10.1016/j.tecto.2011.10.013.

Hooper, A., 2008. A multi-temporal InSAR method incorporating both persistent scatterer and small baseline approaches. GRL, 35, L16302, doi:10.1029/2008GL034654,2008.

Holohan, E. P., Schöpfer, M. P. J., Walsh, J. J., 2011. Mechanical and geometric controls on the structural evolution of pit crater and caldera subsidence. J. Geophys. Res. 116, B07202, doi:10.1029/2010JB008032.

Hutnak, M.S., Hurwitz, S. E., Ingebritsen, Hsieh, P.A., 2009. Numerical models of caldera deformation: Effects of multiphase and multicomponent hydrothermal fluid flow. J. Geophys. Res. 114, B04411, doi:10, 1029/2008JB006151.

Kwoun, O. I., Z. Lu, C. Neal, Wicks, C. Jr., 2006. Quiescent deformation of the Aniakchak Caldera, Alaska mapped by InSAR. Geology, 34, 5 – 8.

Lanari, R., Lundgren, P., Manzo, M., Casu, F., 2004, Satellite radar interferometry time series analysis of surface deformation for Los Angeles, California. Geophys. Res. Lett. 31, L23613, doi:10.1029/2004GL021294.

Lundgren, P., Usai, S., Sansosti, E., Lanari, R., Tesauro, M., Fornaro, G., Berardino, P., 2001. Modeling surface deformation observed with synthetic aperture radar interferometry at Campi Flegrei caldera. J. Geophys. Res., 106, 19,355 – 19,366.

Massonnet, D., Briole, P., Arnaud, A., 1995. Deflation of Mount Etna monitored by spaceborne radar interferometry. Nature, 375, 567 - 570.

Mason B.G, Pyle, D.M., Oppenheimer, C., 2004. The size and frequency of the largest explosive eruptions on Earth. Bull. Volcanol. 66, 735 - 748. doi:10.1007/s00445-004-0355-9.

Massonnet, D., Feigl, K.L., 1998. Radar interferometry and its application to changes in the Earth's surface, Rev. Geophys., 36(4), 441 - 500, doi:10.1029/97RG03139.

McTigue, D. F., 1987. Elastic stress and deformation near a finite spherical magma body: Resolution of the point source paradox. J. Geophys. Res., 92, 12,931 – 12,940.

Merle, O., Borgia, A., 1996. Scaled experiments of volcanic spreading. J. Geophys. Res., 101(B6), 13, 805 – 13, 817.

Montero Lopez, M.C., Hongn, F., Brod, J. F., Seggiaro, R., Marrett, R., Sudo, M., 2010. Magmatismo ácido del mioceno superior-cuaternario en el área de Cerro Blanco-La Hoyada, Puna Austral. Rev. Asoc. Geol. Argent., 67, 3, 329 - 348.

Newhall C G, Dzurisin, D, 1988. Historical unrest at large calderas of the world. U S Geol Surv Bull. 1855 .

Pinel, V., Hooper, A., De la Cruz-Reyna, S., Reyes-Davila, G., Doin, M. P., Bascou, P., 2010. The challenging retrieval of displacement field from InSAR data for andesitic stratovolcanoes : Case study of Popocatepetl and Colima Volcano, Mexico. J. Volc. Geotherm. Res. 200, 49 - 61, doi:10.1016/j.jvolgeores.2010.12.002.

Philibosian, B., Simons, M., 2011. A Survey of Volcanic Deformation on JAVA Using ALOS PALSAR Interferometric Time Series. G-Cubed, 12, Q11004, doi:10.1029/2011GC003775.

Pritchard, M. E., Simons, M., 2002. A satellite geodetic survey of large scale deformation of volcanic centres in the central Andes. Nature, 418, 167 - 170, doi:10.1038/nature00872.

Pritchard, M. E., Simons, M., 2004. An InSAR-based survey of volcanic deformation in the central Andes. Geochem. Geophys. Geosyst. 5, Q02002, doi:10.1029/2003GC000610.

Riller, U., Petrinovic, I., Ramelow, J., Strecker, M., Oncken, O., 2001. Late Cenozoic tectonism, collapse caldera and plateau formation in the central Andes. Earth Planet. Sci. Lett. 188, 299 - 311.

Rosen, P.A., Hensley, S., Joughin, I.R., Li, F.K., Madsen, S.N., Rodriguez, E., Goldstein, R.M., 2000. Synthetic Aperture Radar Interferometry. Proceedings of the IEEE, 88, 3, 333 – 382.

Seggiaro, R., Hongn, F., Folguera, A., Clavero, J., 2000. Hoja Geológica 2769 – II. Paso de San Francisco. Boletín 294. Programa Nacional de Cartas Geológicas. 1:250.000. SEGEMAR.

Sheridan, M. F., Wohletz, K. H., 1983. Hydrovolcanism: Basic considerations and review. J. Volcanol. Geotherm. Res. 17, 1 - 29.

Sigurdsson, H. S., Houghton, B., McNutt, S. R., Rymer, H., Stix, J., 2000. Encyclopedia of Volcanoes. San Diego, Calif. : Academic, c2000.ISBN: 9780126431407.

Simkin, T., L. Siebert, 1994. Volcanoes of the world. Geoscience Press, Tucson, Arizona.

Vilardo, G., Isaia, R., Ventura, G., De Martino, P., Terranova, C., 2010. InSAR Permanent Scatterer analysis reveals fault reactivation during inflation and deflation episodes at Campi Flegrei caldera. Rem. Sens.of Env., 114, 2373 - 2383, doi:10.1016/j.rse.2010.05.014.

Viramonte, J; Castro Godoy, S.; Arnosio, J.; Becchio, Raúl; Poodts, M., 2005 a. El campo geotermal de la caldera del cerro Blanco: utilización de imágenes aster. Actas del Décimo Sexto Congreso Geológico Argentino, 2, 505 - 512.

Viramonte, J., Arnosio, M., Becchio, R., Gropelli, G., Norini, G., Corazzatto, C., DiFillipo, M., Blanco, M., Eulillades, P., Poodts, M., Castro Godoy, S., Klotz, J., Asch, G.y Heit, B., 2005 b. Cerro Blanco Volcanic Complex: the youngest caldera system in the Southern Central Andes. A multidisciplinary Earth Science Project. 19 Colloquium on Latin American Geosciences. Potsdam. Terra Nostra (05/1): 19 LAK Postdam, 135.

Wicks, C., Thatcher, W., Dzurisin, D., Svarc, J., 2006. Uplift, thermal unrest, and magma intrusion at Yellowstone caldera, observed with InSAR. Nature, 440, 72 - 75, doi:10.1038/nature04507.

Zebker, H. A., Villasenor J., 1992. Decorrelation in interferometric radar echoes, IEEE Trans. Geosci. Remote Sens., 30, 950 - 59.

Zebker, H.A., Rosen, P.A., Hensley, S., 1997. Atmospheric effects in interferometric synthetic aperture radar surface deformation and topographic maps. J. Geophys. Res., 102(B4), 7547 - 7563.

Zhou, X; Chang, N.-B., Li, S, 2009. Applications of SAR Interferometry in Earth and Environmental Science Research. Sensors, 9, 1876 - 1912; doi:10.3390/s90301876.

Captions

Fig. 1: a) Geologic map of the studied area (modified after Montero Lopez et al., 2010). The red rectangle refers to the studied area by SAR techniques as reported in Fig. 1b, 2, 3 and 4. b) Topography and main features of CBCR area: CBC - Cerro Blanco Caldera; RC - Robledo Caldera; CBRC - Cerro Blanco/Robledo Caldera (black circle envelope the whole volcanic structure); CPP - Campo de la Piedra Pomez; EN - El Niño volcanic structure; LH - La Hoyada Volcanic Complex; LP - Laguna Purulla Black dashed line is the trace of valley in the LP area, convex towards the northwest (see the text for description).

Fig.2: Surface velocity map, related to the time period April 2003 and January 2007 (ENVISAT dataset), obtained by applying the A-InSAR method of StaMPS-MTI. The red diamonds indicates the point assumed as reference, i.e. with zero deformation.

Fig.3: Map of the deformation (ASAR/ENVISAT) measured in the time span between August 2005 and June 2010 by means of differential InSAR. A circular pattern, with a maximum negative value of about -4.3 cm, is highlighted in the map. The results confirm the analysis preformed by using StaMPS-MTI method.

Fig.4: Map of the deformation obtained by differential InSAR applied to the ERS2 images pair (May 16/5/1996-12/10/2000). The maximum subsidence is of about 8 cm, with a circular shape centered just after the ridge separating Cerro Blanco and Robledo calderas, towards south-east.

Fig. 5: Profiles of the measured deformations. Left axis of the plots report the deformation and the right axis to the elevation values, respectively. The inset reports the shaded relief of the area and the three analyzed transects. Continuous lines are related to the reference topography; dot lines refer to ENVISAT differential InSAR; dashed lines are related to ERS2 data, and points cloud refer to the equivalent deformation (cumulative) of A-InSAR data obtained by multiplying the LOS mean

velocity for the period of observation (i.e. 4.4 years). On the x-axis the crossing points of the transects are also reported.

Fig. 6: Trend of LOS deformation rates with respect to time. The four segments in the plot refer to the four time period analyzed by InSAR data. Continuous line segments are related to single interferogram approach (standard InSAR), while dashed line segment corresponds to SAR time series, i.e. StaMPS-MTI approach. Segment A (from Pritchard et al., 2004) reports a deflation velocity of about 2.6 cm/yr measured with ERS descending data; for segment B (from Pritchard et al. 2004) 1.8 cm/yr have been calculated (ERS descending data); segment C and D segments are related to ENVISAT descending (C) and ascending (D) data analysis, which show values of 1.2 cm/yr and 0.87 cm/yr, for C and D respectively. The plot clearly point out the decreasing trend of the surface velocity.

Figure 1a
Click here to download high resolution image

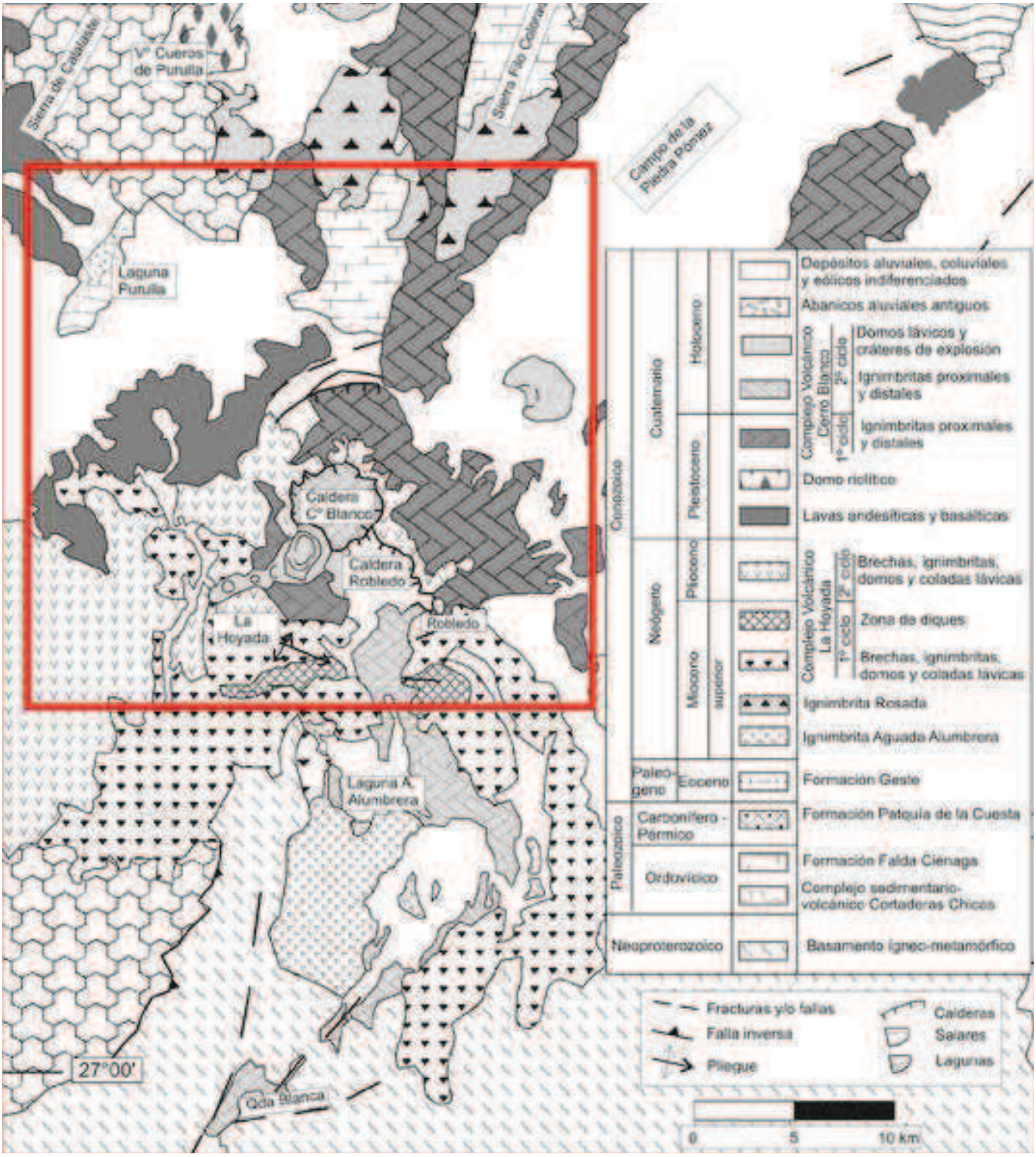

Figure 1b

Click here to download high resolution image

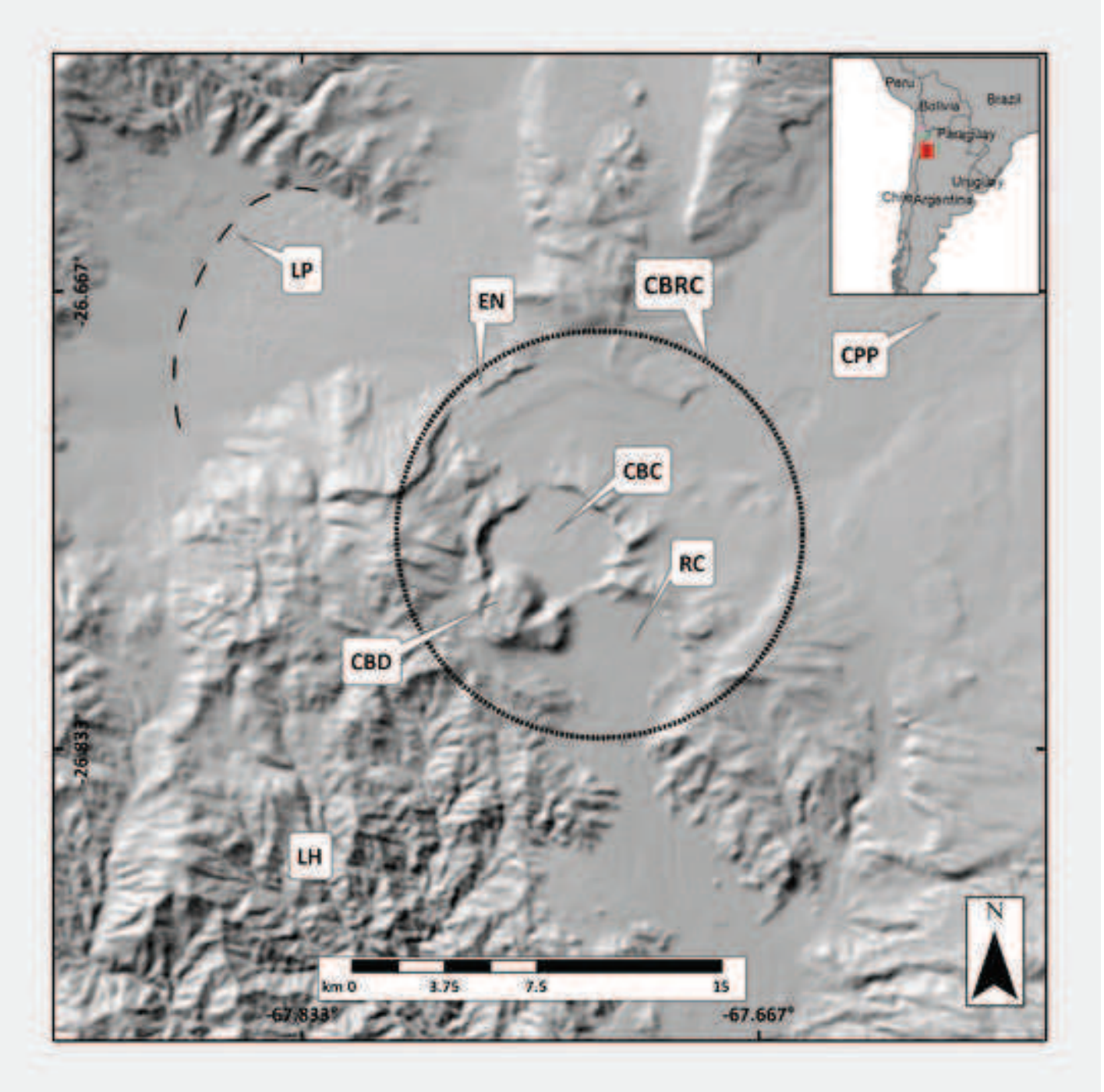

Figure 2
Click here to download high resolution image

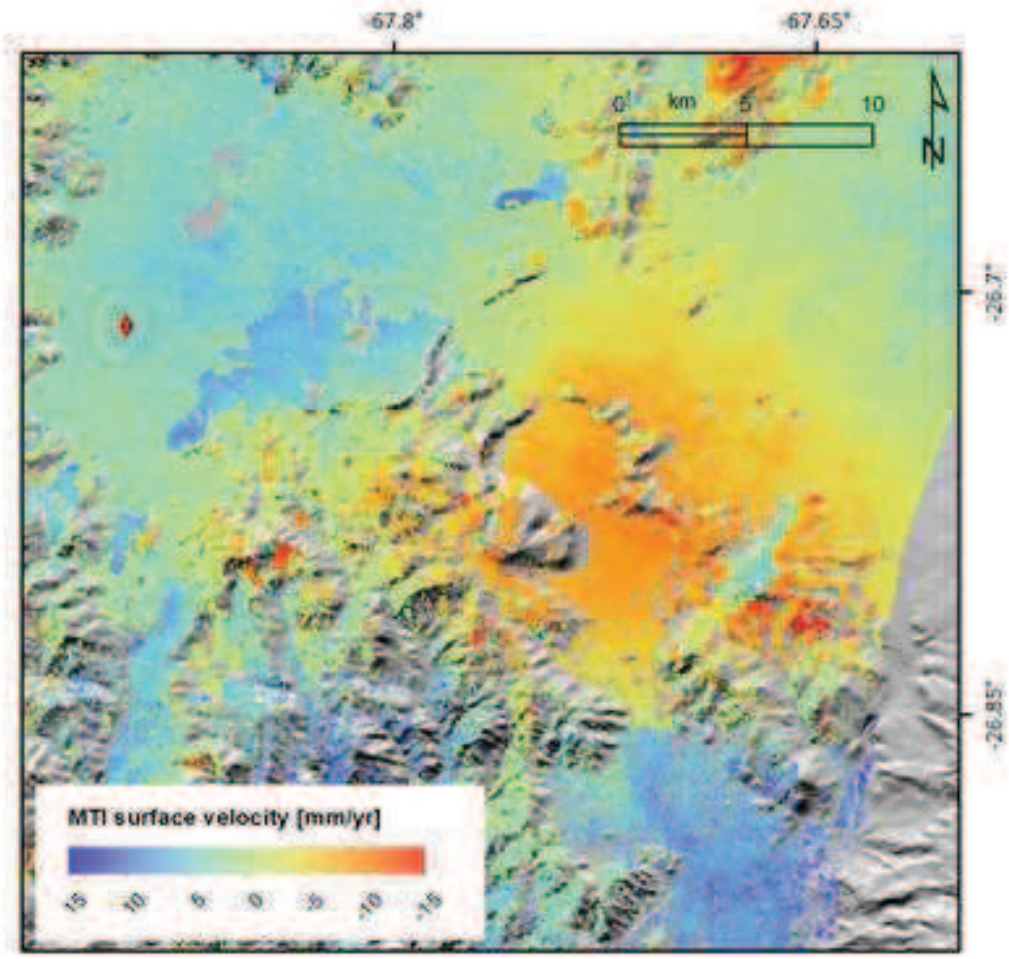

Figure 3
Click here to download high resolution image

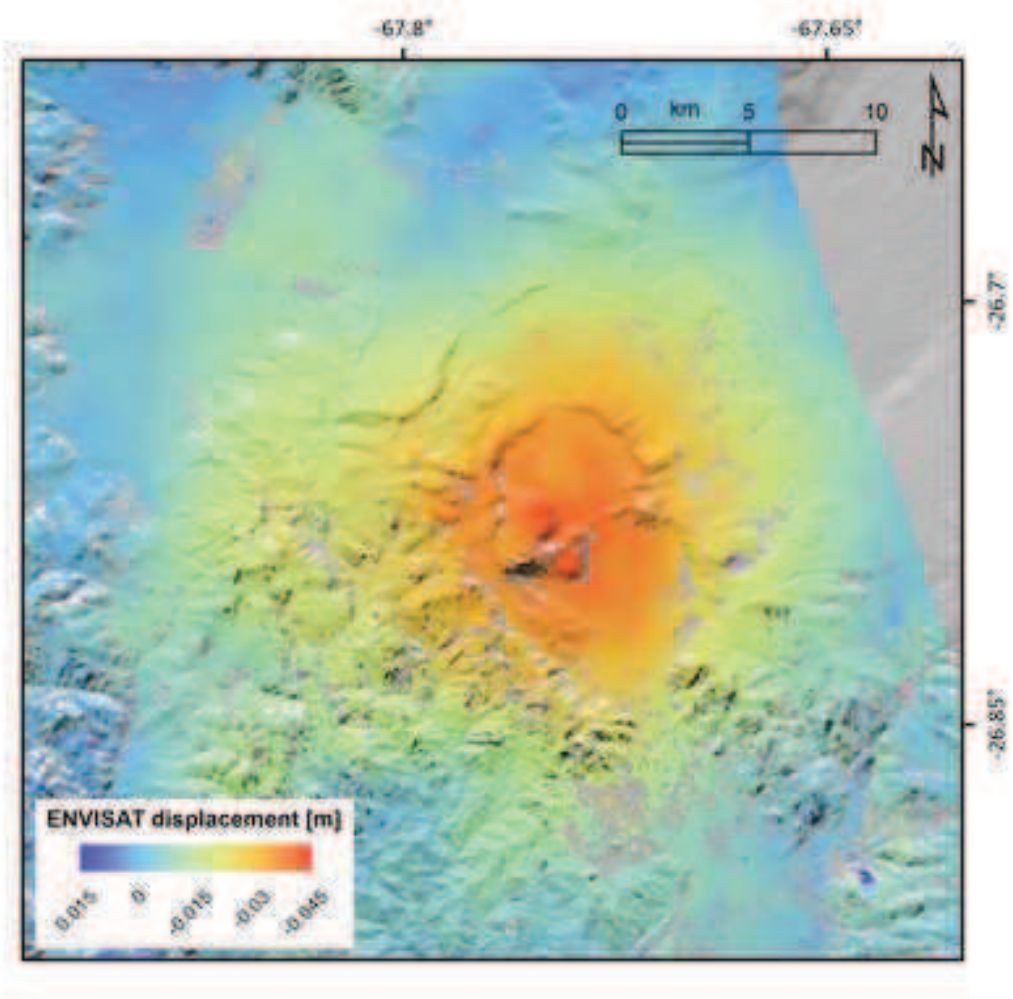

Figure 4
Click here to download high resolution image

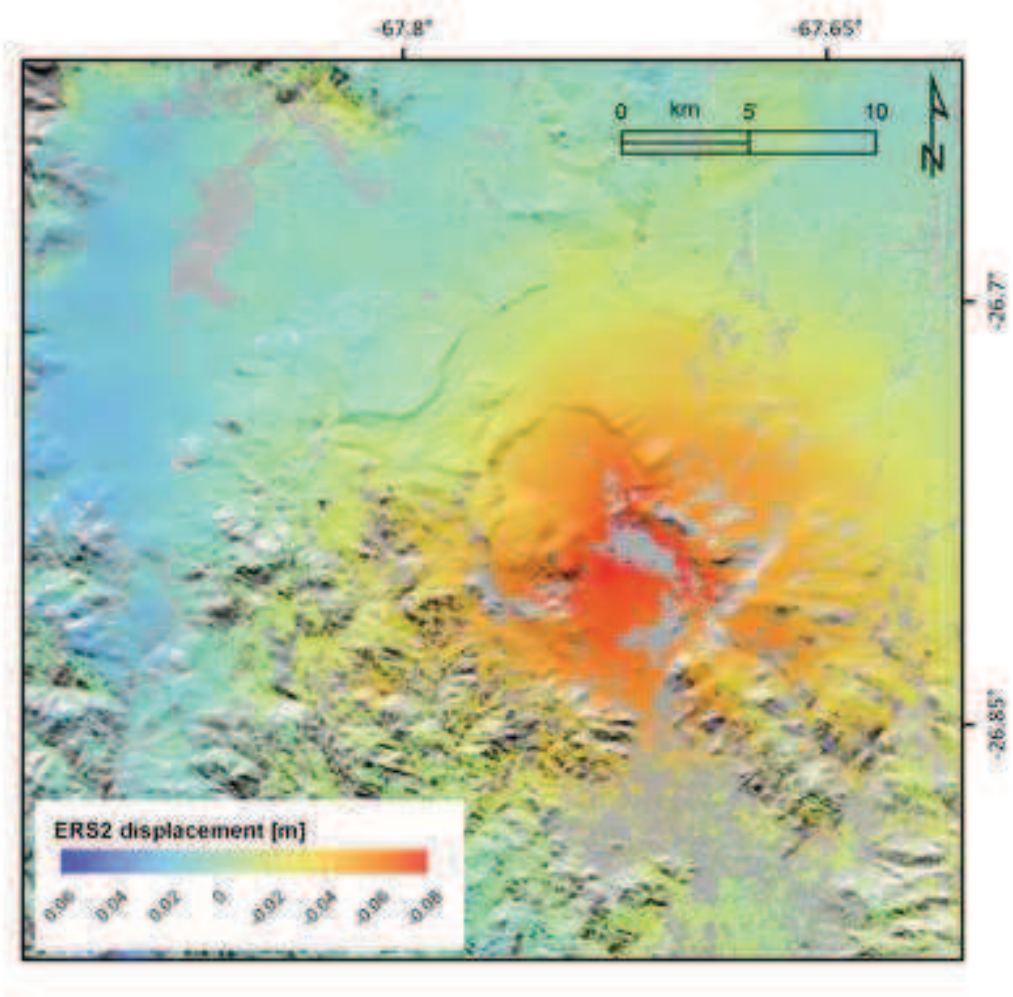

Figure 5

Click here to download high resolution image

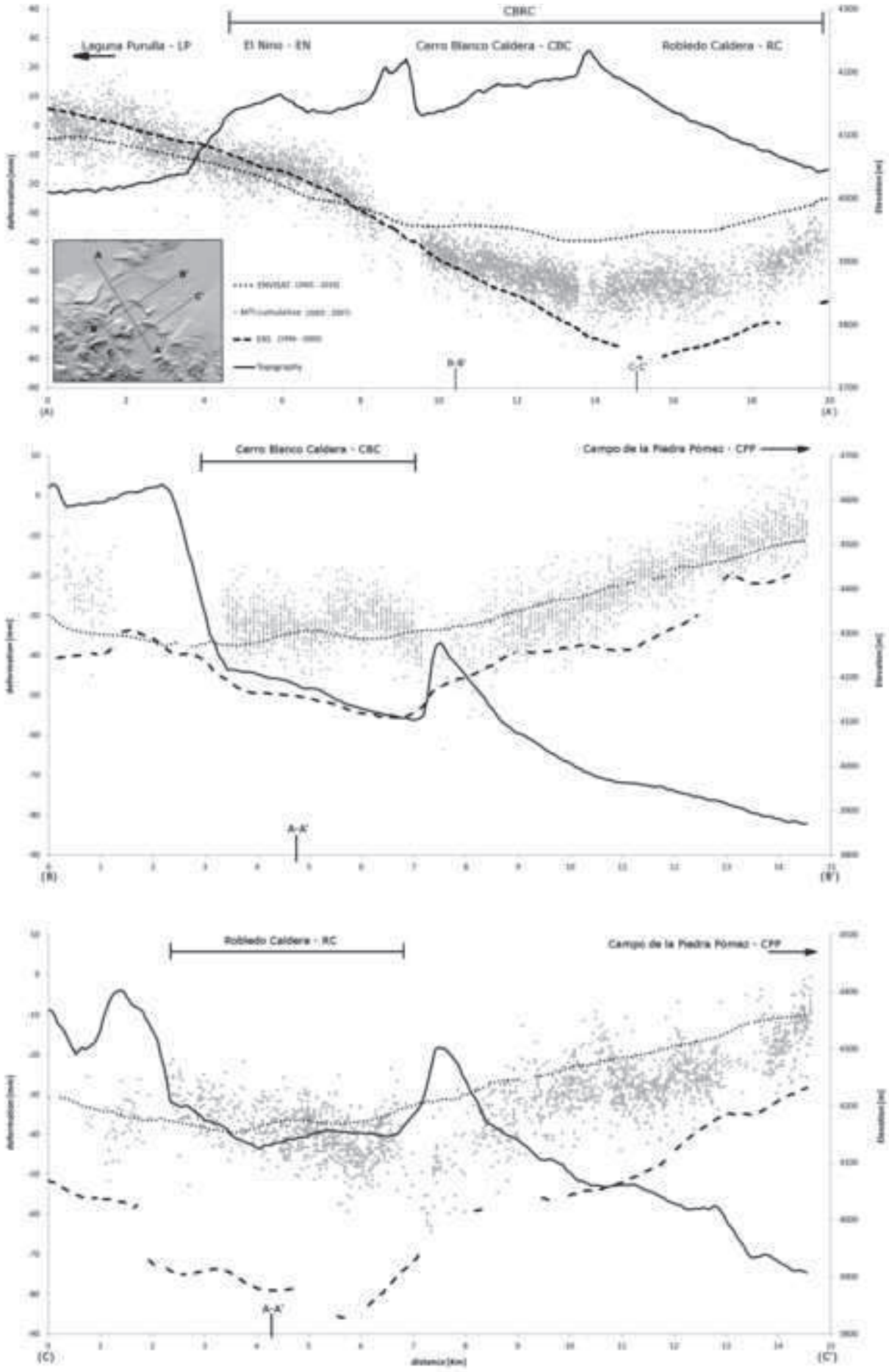

Figure 6
Click here to download high resolution image

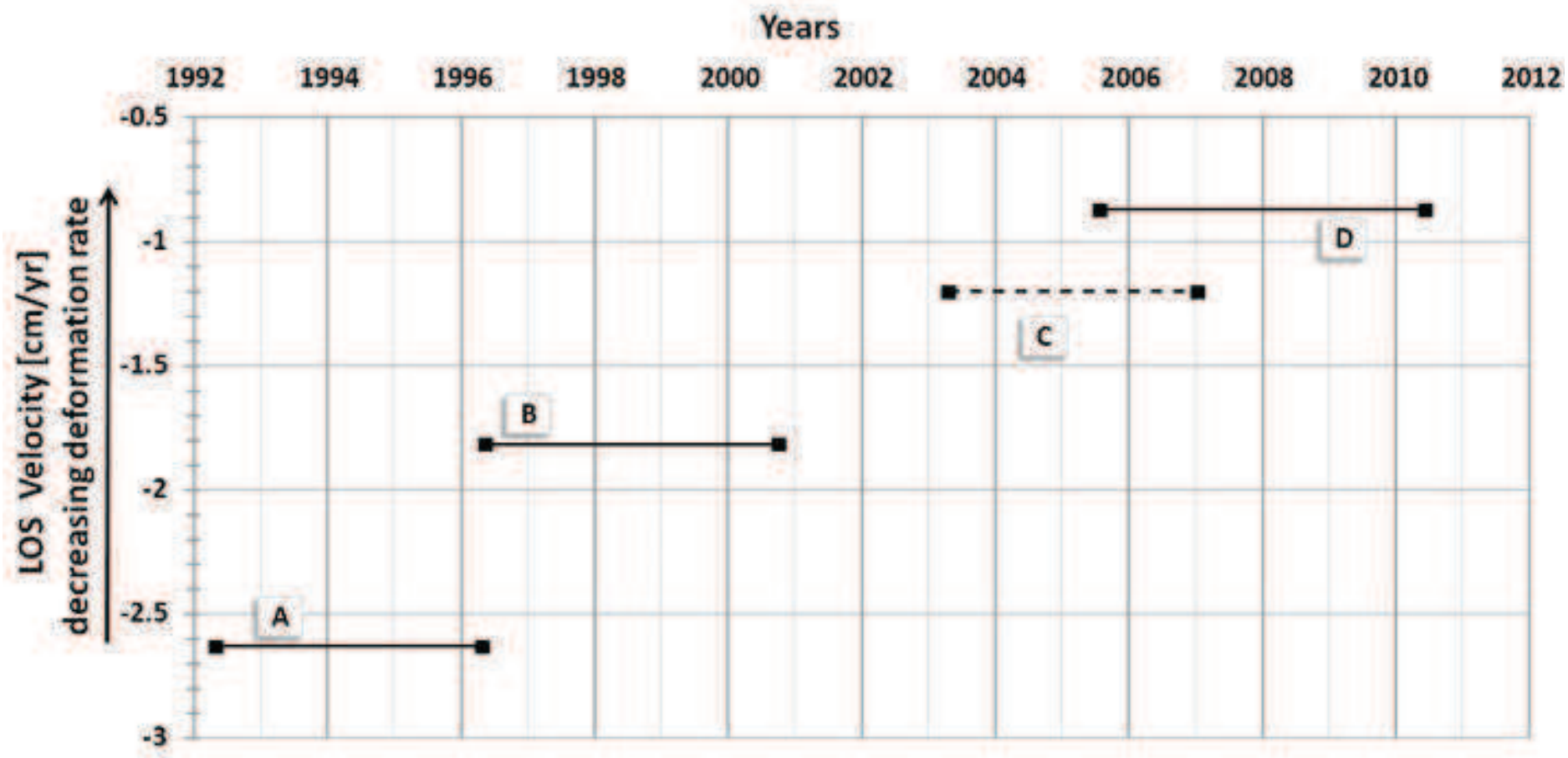

Table

Satellite	Caldera subsidence mean-velocity
ENVISAT descending track 10 - SAR time series	1.8 cm/yr
29/04/2003	
08/07/2003	
13/04/2004	
09/11/2004	
14/12/2004	
18/01/2005	
22/02/2005	
29/03/2005	
07/06/2005	
12/07/2005	
25/10/2005	
07/02/2006	
23/01/2007	
ENVISAT ascending track 318 - InSAR	1.2 cm/yr
03/08/2005	
23/06/2010	
ERS2 descending track 239 - InSAR	0.87 cm/yr
16/05/1996	
12/10/2000	

Table 1: List of the processed images from ENVISAT and ERS satellites and relative average velocities of maximum CBRC subsidence.